MEDICAL SCIENCE MONITOR

ANIMAL STUDY

e-ISSN 1643-3750
© Med Sci Monit, 2020; 26: e923049
DOI: 10.12659/MSM.923049

Received: 2020.01.23
Accepted: 2020.04.20
Available online: 2020.05.23
Published: 2020.07.20

Protective Effects of Ischemic Postconditioning on Livers in Rats with Limb Ischemia-Reperfusion via Glycogen Synthase Kinase 3 beta (GSK-3β)/Fyn/Nuclear Receptor-Erythroid-2-Related Factor (Nrf2) Pathway

Authors' Contribution:
Study Design A
Data Collection B
Statistical Analysis C
Data Interpretation D
Manuscript Preparation E
Literature Search F
Funds Collection G

CDEF Qibing Niu*
BCDEF Wanli Sun*
AEG Quan Chen
EF Yang Long
BC Wanjun Cao
BC Shiqi Wen
DE Anqiang Li
BE Fang Dong
EF Hao Shi

Department of Vascular Surgery, People's Hospital in Gansu Province, Gansu University of Chinese Medicine, Lanzhou, Gansu, P.R. China

* Qibing Niu and Wanli Sun contributed equally to this work

Corresponding Author: Quan Chen, e-mail: chenquan012@163.com
Source of support: Departmental sources

Background: Ischemia/reperfusion (I/R) injury not only exists in ischemic tissues and organs, but also can cause damage to distant tissues and organs. As the largest metabolic organ of the human body, the liver is very vulnerable to injury after limb I/R. However, the mechanism of liver injury caused by limb I/R injury has not been fully elucidated. This study investigated the effect and mechanism of ischemic postconditioning (IPO) on the liver after hindlimb I/R in rats.

Material/Methods: A rat model of hindlimb I/R was established and treated by IPO. Liver function, changes of oxidative stress index and inflammation, Bcl-2 and Bax proteins, and apoptosis were assessed. The structural changes were observed by electron microscopy. GSK-3β/Fyn/Nrf2 levels were detected by quantitative PCR and Western blot.

Results: IPO significantly reduced serum AST, ALP, LDH, and ALT levels induced by I/R. Compared with the I/R group, the levels of SOD, GSH-Px, and CAT in the IPO group were significantly increased, while the levels of MDA, MPO, and ROS were significantly decreased. The IPO group had significantly higher Bcl-2 level and significantly lower Bax level compared to the I/R group. Consistently, IPO decreased the apoptosis rate induced by I/R. Furthermore, IPO lowered the levels of TNF-α, IL-1β, IL-10, and INF-γ and alleviated the ultrastructural changes of hepatocytes. Finally, Nrf2, Fyn, and GSK-3β mRNA and protein levels in the IPO group were significantly higher than in the I/R group.

Conclusions: IPO protects against liver injury caused by I/R injury of the hindlimb, possibly via the GSK-3β/Fyn/Nrf2 pathway.

MeSH Keywords: Glycogen Synthase Kinase 3 • Ischemic Attack, Transient • Ischemic Postconditioning • Ischemic Preconditioning • Proto-Oncogene Proteins c-fyn • Reperfusion Injury

Full-text PDF: https://www.medscimonit.com/abstract/index/idArt/923049

Indexed in: [Current Contents/Clinical Medicine] [SCI Expanded] [ISI Alerting System] [ISI Journals Master List] [Index Medicus/MEDLINE] [EMBASE/Excerpta Medica] [Chemical Abstracts/CAS]

Background

Surgery, embolism, trauma, and iatrogenic arterial injury can cause severe acute limb ischemia, and can cause injury to distal organs and tissues such as the heart, lungs, liver, and kidneys [1]. Limb ischemia-reperfusion (I/R) can cause liver injury, which is common in liver transplantation, low-volume shock, trauma, and burns. Such liver injury can reduce liver metabolism and detoxification ability, increase microcirculation resistance, and even lead to liver failure and affect the function of distant organs [2]. Thus, it is of great importance to study the pathophysiological mechanism of liver injury induced by limb I/R and to develop strategies to prevent liver injury caused by limb I/R.

I/R injury of limbs is a complex cascade reaction, which is currently considered to be related to the production of oxygen free radicals [3], calcium overload [4], neutrophils and inflammatory factors [5], activation of Kupffer cells [6], microcirculation disorders [7], energy metabolism disorders [8], and cell apoptosis [9]. It is confirmed that the mechanism of limb I/R injury to distant tissues and organs is closely related to oxygen free radicals and polymorphonuclear neutrophil (PMN). During limb I/R injury, a large number of oxygen free radicals are produced. These oxygen free radicals can cause lipid peroxidation in liver cell membrane, mitochondrial membrane, microsomal membrane, and lysosomal membrane. They act directly on endothelial cell membranes of hepatic sinusoids and increase the attachment and aggregation of neutrophils and platelets, leading to microcirculation disturbance [10,11]. Additionally, they can oxidize nuclease, break double chains, and eventually lead to necrosis of hepatocytes [12]. After the activation of Kupffer cells by limb I/R injury, they release a variety of inflammatory cytokines, such as tumor necrosis factor-α (TNF-α), interleukin (IL), platelet activating factor, and leukotriene, which can induce aggregation of neutrophils, promote the adhesion of leukocytes and platelets to the endothelial cells of hepatic sinusoids, and aggravate the endothelium [13, 14]. Cell damage and disorder of microcirculation in the liver can also induce the formation of prostaglandins and nitric oxide and ultimately initiate I/R liver injury after warm or cold ischemia [15].

Murry et al. [16] put forward the concept of ischemic preconditioning (IPC) in 1986, which suggests that the short-term reperfusion of ischemic myocardium can significantly improve myocardial I/R injury. Many studies have shown that IPC can be used to alleviate I/R injury of various tissues and organs in many animals [17–19]. However, the clinical value of IPC is limited because it is difficult to estimate the time of ischemia of tissues and organs in clinical practice. In 2003, Zhao et al. [20] first discovered that ischemic postconditioning (IPO) can alleviate I/R injury by reducing the aggregation of neutrophils. In IPO, several short perfusion-blocking cycles after organ ischemia and before reperfusion are implemented to attenuate reperfusion-induced injury. Previous studies have confirmed that prevention of I/R liver injury can be achieved by inhibiting hepatocyte apoptosis and protecting liver mitochondrial function [21,22]. IPO can be implemented after ischemia. Thus, its clinical controllability is strong, and it has more important clinical value and significance. However, the protective effect of IPO on liver injury induced by limb I/R is not well studied, and the specific mechanism is not clear.

Nuclear receptor-erythroid-2-related factor (Nrf2) is a basic region of leucine zipper transcription factor, which has the function of regulating the expression of a series of oxidation-related genes [23,24]. It has been found that GSK-3β is involved in the regulation of oxidative stress and is involved in regulation of Nrf2 system activity by Fyn [25]. Fyn is a member of the Scr tyrosine protein kinase family. After activation, it can enter the nucleus and exports out the nucleus Nrf2. After ubiquitination, it is degraded by protease [26]. It has been reported that Nrf2, GSK-3β, and Fyn signal pathways play an important role after I/R injury [27–29], but it is not clear whether they are involved in the occurrence and development of liver injury after limb I/R.

The present study investigated the protective effect of IPO on livers of rats with limb I/R. The possible role of GSK-3β/Fyn/Nrf2 pathway was also analyzed and discussed.

Material and Methods

Laboratory animals

Thirty-two healthy male SD rats, weighing 220–250 g, age 6 to 7 weeks, were purchased from Shanghai Slek Laboratory Animal Co. with the certificate number SCXK (Shanghai) 2018-0005. They were kept at a constant temperature (24±1°C), with 4 rats per cage, dark/light cycle of 12 h, and free access to standard rat chow and drinking water. The experiments were conducted after 1 week of adaptive feeding. All animal studies conformed to the National Regulations on the Administration of Laboratory Animals. All animal procedures were approved by the Ethics Committee of Gansu University of Chinese Medicine.

Reagents

Superoxide dismutase (SOD), malondialdehyde (MDA), myeloperoxidase (MPO), glutathione peroxidase (GSH-Px), catalase (CAT), and reactive oxygen species (ROS) kits were purchased from Nanjing Jiancheng Institute of Bioengineering (Nanjing, China). Lactate dehydrogenase (LDH) kits were purchased from Shanghai Beyotime Biotechnology Co. (Shanghai, China). Tumor necrosis factor-α (TNF-α), Interleukin-1 β (IL-1β),

Indexed in: [Current Contents/Clinical Medicine] [SCI Expanded] [ISI Alerting System] [ISI Journals Master List] [Index Medicus/MEDLINE] [EMBASE/Excerpta Medica] [Chemical Abstracts/CAS]

Interleukin-10 (IL-10), and Interferon-γ (IFN-γ) kits were purchased from Changzhou Dimenuo Biotechnology Co., (Changzhou, China). TUNEL cell apoptosis detection kits were purchased from Shanghai Beyotime Biotechnology Co. (Shanghai, China). *In situ* cell apoptosis detection kits were purchased from ROCHE (Switzerland). DAB Detection kits were purchased from Bohai Bioengineering Co. (Hebei, China). Antibodies against Bcl-2 (cat# 60178-1-Ig), Bax (cat# 60267-1-Ig), GSK-3β (cat# 67329-1-Ig), Fyn (cat# 66606-1-Ig), Nrf2 (cat# 66504-1-Ig), and β-actin (cat# 60008-1-Ig) were all purchased from Proteintech Co. (Chicago, USA). HRP-labeled goat anti-mouse IgG antibody was purchased from Santa Cruz Co. (cat# sc-2005; Santa Cruz, California, USA). The reverse transcription kits were purchased from TransGen Biotech Co., (Beijing, China). RT-PCR kits and Western blot kits were purchased from Semerfly Technology Co. (Shanghai, China).

Establishment of model and animal grouping [30]

The I/R injury model was established in hindlimbs of rats. Briefly, rats were fasted for 12 h before the operation. Under shallow anesthesia with ether, rats were ligated around the root of their hind limbs with rubber bands. After ligation, pale and cool toes were observed. No arterial pulsation was observed at the distal end. No blood flow signals were detected by laser Doppler flow imaging. After ligation for 4 h, the blood flow was released and blood perfusion was performed for 6 h. Before release and ligation, 10% chloral hydrate (3 mL/kg) was injected into the abdominal cavity, and 1000 U/kg heparin was injected into the penile vein for anticoagulation. The animals were randomly divided into 4 groups, with 8 rats in each group. The Sham operated (SO) group received only anesthesia, with the hind limb relaxed around the rubber band, and without blocking blood flow. The I/R group received ischemia for 4 h and reperfusion for 6 h. In the IPC group, the blood flow of both hind limbs was pre-blocked for 5 min and then re-perfused for 5 min, the procedure was repeated for 3 times, and the other procedures were the same as in the I/R group. In the IPO group, after blocking the blood flow for 4 h, the femoral artery of both hind limbs was ligated for 1 min and then re-perfused for 1 min, the procedure was repeated for 3 times, and the other procedures were the same as in the I/R group. After 6 h of reperfusion, rats in each group were anesthetized by intraperitoneal injection of 10% chloral hydrate (0.3 mL/100 g body weight). We collected 2 mL of blood through the abdominal aorta. The liver was quickly removed for further analysis. The modeling process was carried out at room temperature.

Determination of plasma biochemical parameters

Serum was collected from blood by centrifugation at 3000 r/min for 15 min. The levels of aspartate aminotransferase (AST), alanine aminotransferase (ALT), and alkaline phosphatase (ALP) in serum were measured by automatic biochemical analyzer, and the level of LDH was assessed using an LDH kit.

ELISA

ELISA was used to detect changes in oxidative stress parameters in rat livers, including SOD, MDA, MPO, GSH-Px, CAT, and ROS, and to measure the expression levels of TNF-α, IL-1β, IL-10, and interferon gamma (INF-γ) in liver tissues. The procedure was performed with corresponding kits according to the kit instructions.

Immunohistochemistry

Expression of Bcl-2 and Bax in liver tissue was detected with immunohistochemical method. Briefly, the rat liver was fixed with 4% paraformaldehyde. Paraffin-embedded tissues were cut into 5-μm-thick sections. Routine immunohistochemistry assessment was performed. Color development was performed with DAB staining. Bcl-2- and Bax-positive staining was shown as brown granules in the nuclear membrane and cytoplasm of hepatocytes. The number of cells with positive staining was counted under 5 randomly selected high-power visual fields. The percentage of positive cells out of the total number of cells was calculated.

Cell apoptosis assay

TUNEL method was used to detect hepatocyte apoptosis by TRITC staining according to the instructions of the kit. Eight sections were randomly selected from each group. The number of apoptotic cells and the total number of cells were counted under 5 high-power fields (×400). The apoptosis index was calculated as (apoptotic cell number/total cell number)×100%.

Electron microscope observation

The rat liver was fixed by 4% polyformaldehyde, cut into 1-mm^3 pieces, fixed, dehydrated, and embedded using the conventional osmium acid method, and ultrathin sections were prepared by positioning the thick slices, and the ultrastructural changes of hepatocytes in each group were observed under an electron microscope.

Reverse transcription-quantitative polymerase chain reaction (RT-qPCR)

Total RNA was extracted from liver tissues by Trizol reagent. The purity of RNA was detected by ultraviolet spectrophotometer at 260 nm. Reverse transcription and RT-qPCR were performed according to the directions of the reverse transcription and PCR kits (Applied Biosystems; Thermo Fisher Scientific, Inc.). The conditions of RT-qPCR reaction were as follows: 94°C

Indexed in: [Current Contents/Clinical Medicine] [SCI Expanded] [ISI Alerting System] [ISI Journals Master List] [Index Medicus/MEDLINE] [EMBASE/Excerpta Medica] [Chemical Abstracts/CAS]

Table 1. Primer sequences.

	Primer sequence
GSK-3β	Forward 5'-GGT GAC TTT GAC CGG AAC GTG-3'
	Reserve 5'-ATT GAA GGG ACA GGT GAA CAG G-3'
Fyn	Forward 5'-CAC AGG GTG ACA GAA GAG GCT AA-3'
	Reserve 5'-ACA CTC CCT GAG ACC AGA AAC AC-3'
Nrf2	Forward 5'-GCG GTG AGA AGA GCC CTG AT-3'
	Reserve 5'-GCT CCC CTG TGA TGT CGT TTC-3'
U6	Forward 5'-CGC CAG TAG ACT CCA CGA CAT A-3'
	Reserve 5'-AAG TTC AAC GGC ACA GTC AAG G -3'

pre-denaturation for 5 min, 40 cycles of denaturation at 96°C for 30 s, annealing at 60°C for 40 s, and elongation at 72°C for 1 min, and final elongation at 72°C for 10 min. The primer sequences of RT-qPCR reaction are shown in Table 1. U6 was used as the internal reference. The PCR products were analyzed by electrophoresis and the results were analyzed by Opticon Monitor 3 software. The experiment was repeated 3 times and the average value was calculated.

Western blot analysis

Total proteins were extracted from liver tissues. The BCA protein detection kit was used to determine the protein concentration. We separated 100 mg of protein by 10% SDS-PAGE electrophoresis and transferred it to PVDF membranes. At room temperature, the membrane was blocked with 5% non-fat milk for 1 h. Then, primary antibodies anti-GSK-3β (1: 1000), anti-Fyn (1: 1000), anti-Nrf2 (1: 500), and anti-β-actin (1: 500) were added and incubated overnight at 4°C. After washing with PBST 3 times, the secondary antibody (1: 200) was added for incubation. Color development was performed with chemiluminescence. The optical densities of bands were quantified using Gel-Pro Analyzer software version 4.0 (Media Cybernetics, Inc., Rockville, MD, USA). β-actin was used as the endogenous control.

Statistical analysis

All the data were analyzed by SPSS 13.0 medical statistical software (SPSS Inc., Chicago, IL, USA). The experimental data were expressed by mean±standard deviation. One-way ANOVA with complete random design was used. The Student-Newman-Keuls

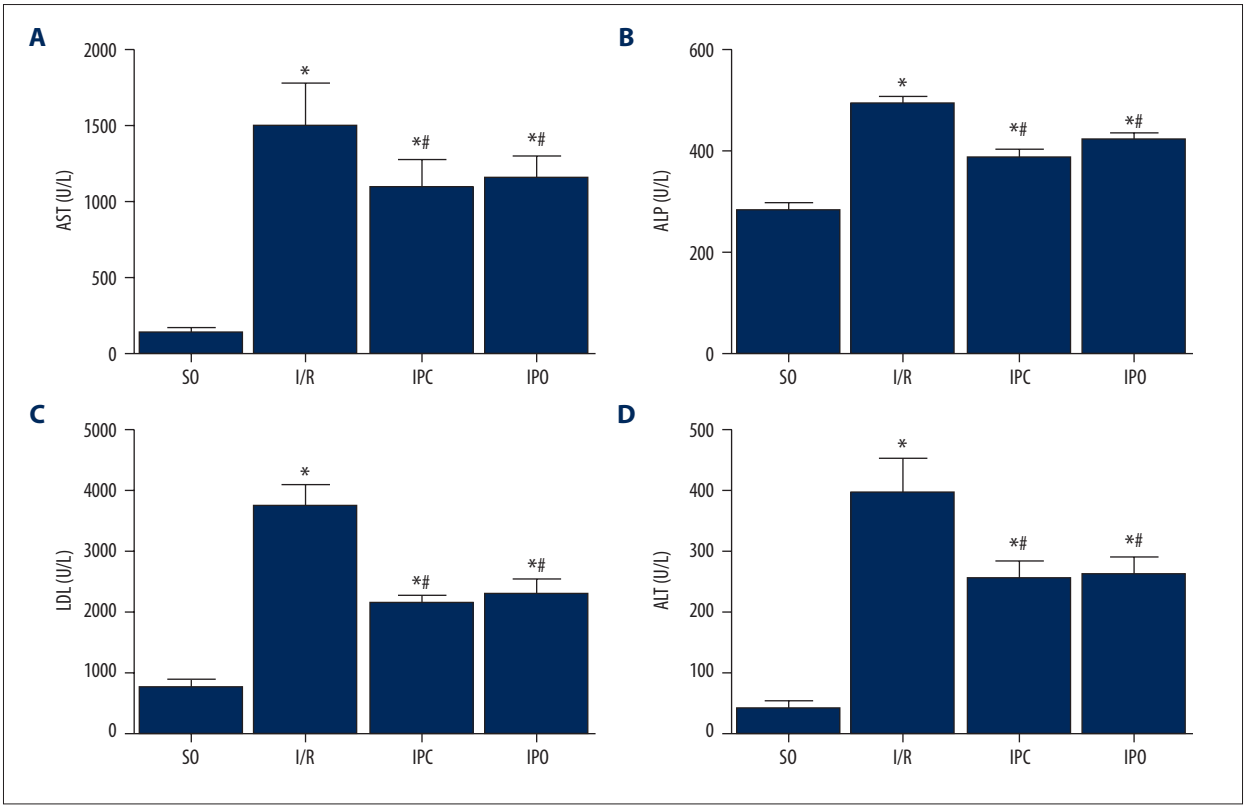

Figure 1. Changes in ALT, AST, ALP, and LDH levels in serum. Rats were divided into the SO group, I/R group, IPC group, and IPO group. The levels of (**A**) AST, (**B**) ALP, (**C**) LDH, and (**D**) ALT in serum were detected. Compared with SO, * P<0.05; compared with I/R, # P<0.05.

Indexed in: [Current Contents/Clinical Medicine] [SCI Expanded] [ISI Alerting System] [ISI Journals Master List] [Index Medicus/MEDLINE] [EMBASE/Excerpta Medica] [Chemical Abstracts/CAS]

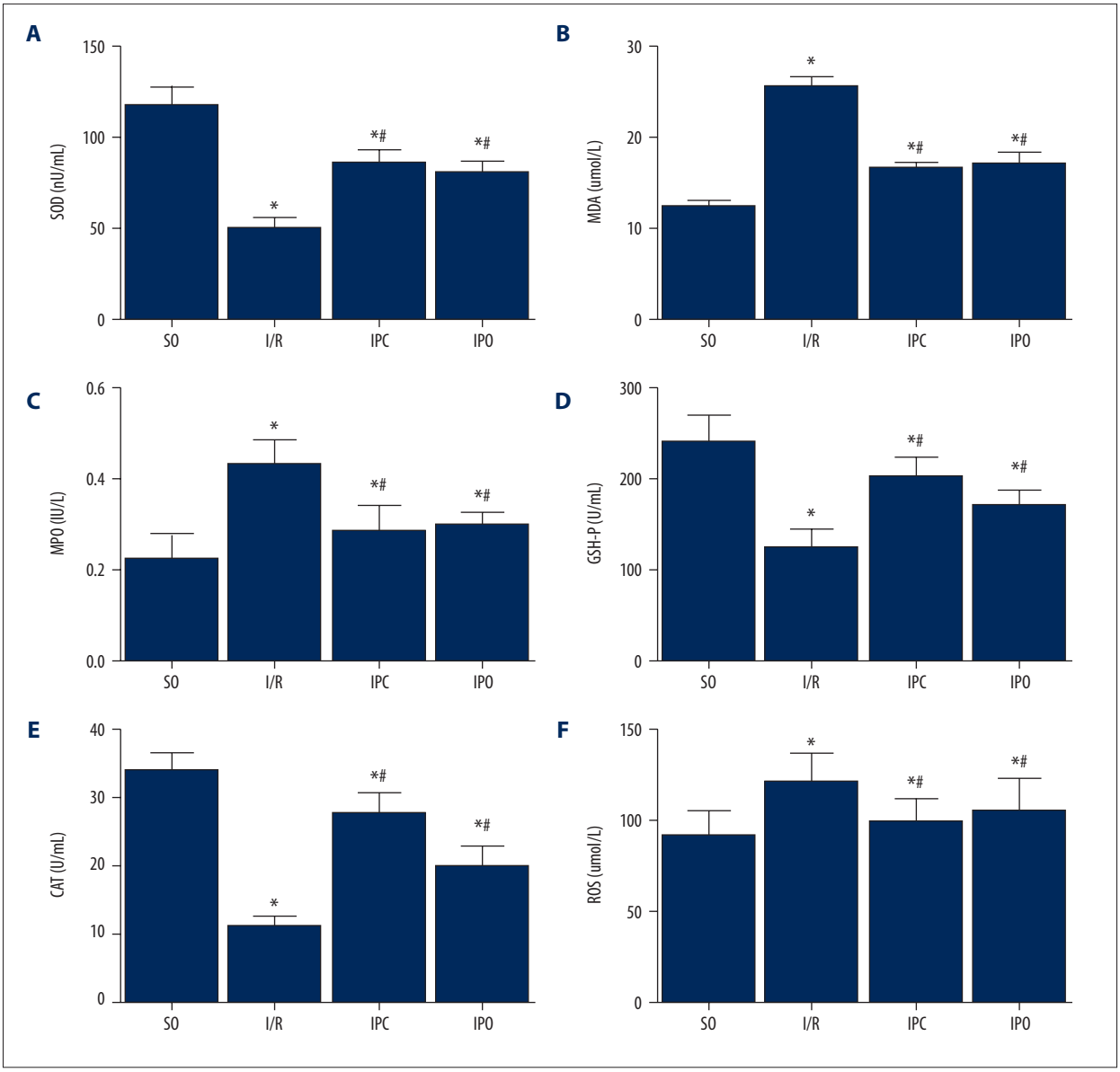

Figure 2. Changes in oxidative stress index in liver tissue. Rats were divided into the SO group, I/R group, IPC group, and IPO group. The levels of (**A**) SOD, (**B**) MDA, (**C**) MPO, (**D**) GSH-Px, (**E**) CAT, and (**F**) ROS in liver tissue were detected with ELISA. Compared with SO, * P<0.05; compared with I/R, # P<0.05.

Q test was used to compare the 2 mean values of multiple samples. The difference was statistically significant at P<0.05.

Results

Changes in ALT, AST, ALP, and LDH levels in serum

The serum levels of liver function indicators were analyzed. Compared with the SO group, the contents of serum AST (Figure 1A), ALP (Figure 1B) LDH (Figure 1C), and ALT (Figure 1D) in the I/R, IPC, and IPO groups increased significantly (P<0.05). Compared with group I/R, the levels of serum AST (Figure 1A), ALP (Figure 1B), LDH (Figure 1C), and ALT (Figure 1D) in the IPC and IPO groups were significantly decreased (P<0.05), but there was no significant difference between the IPO and IPC groups (P>0.05).

Changes in oxidative stress index in liver tissue

To determine the changes in oxidative stress index, ELISA was performed. Compared with the SO group, the levels of SOD (Figure 2A), GSH-Px (Figure 2D), and CAT (Figure 2E) in liver tissue of the I/R, IPC and IPO groups decreased significantly, while the

Indexed in: [Current Contents/Clinical Medicine] [SCI Expanded] [ISI Alerting System] [ISI Journals Master List] [Index Medicus/MEDLINE] [EMBASE/Excerpta Medica] [Chemical Abstracts/CAS]

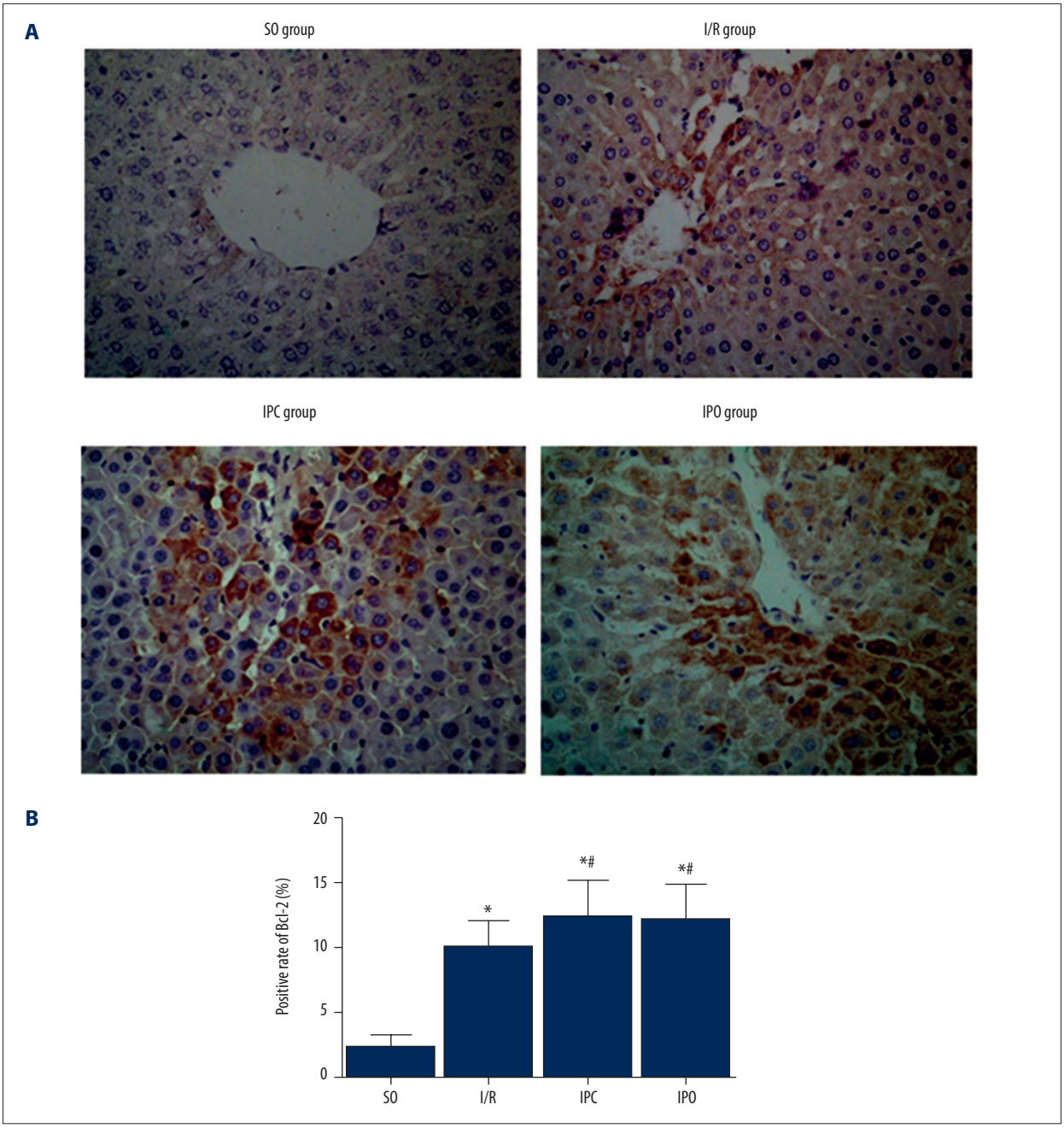

Figure 3. Level of Bcl-2 protein in liver tissue. Rats were divided into the SO group, I/R group, IPC group, and IPO group. Bcl-2 level was detected with immunohistochemistry. (**A**) Representative immunohistochemical staining results of Bcl-2 in SO group, I/R group, IPC group, and IPO group are shown. (**B**) Positive rate of Bcl-2. Compared with SO, * P<0.05; compared with I/R, # P<0.05.

levels of MDA (Figure 2B), MPO (Figure 2C), and ROS (Figure 2F) increased significantly (P<0.05). Compared with the I/R group, the levels of SOD (Figure 2A), GSH-Px (Figure 2D), and CAT (Figure 2E) in the IPO and IPC groups significantly increased, while the levels of MDA (Figure 2B), MPO (Figure 2C), and ROS (Figure 2F) significantly decreased (P<0.05). However, no significant difference was found between the IPO and IPC groups (P>0.05).

Level of Bcl-2 protein in liver tissue

To determine the Bcl-2 level in liver tissue, immunohistochemistry was conducted. Representative immunohistochemical staining results are shown in Figure 3A. The results showed that the positive rate of Bcl-2 in the IPC group and IPO group was obviously higher than that in the I/R group. Statistically,

Indexed in: [Current Contents/Clinical Medicine] [SCI Expanded] [ISI Alerting System] [ISI Journals Master List] [Index Medicus/MEDLINE] [EMBASE/Excerpta Medica] [Chemical Abstracts/CAS]

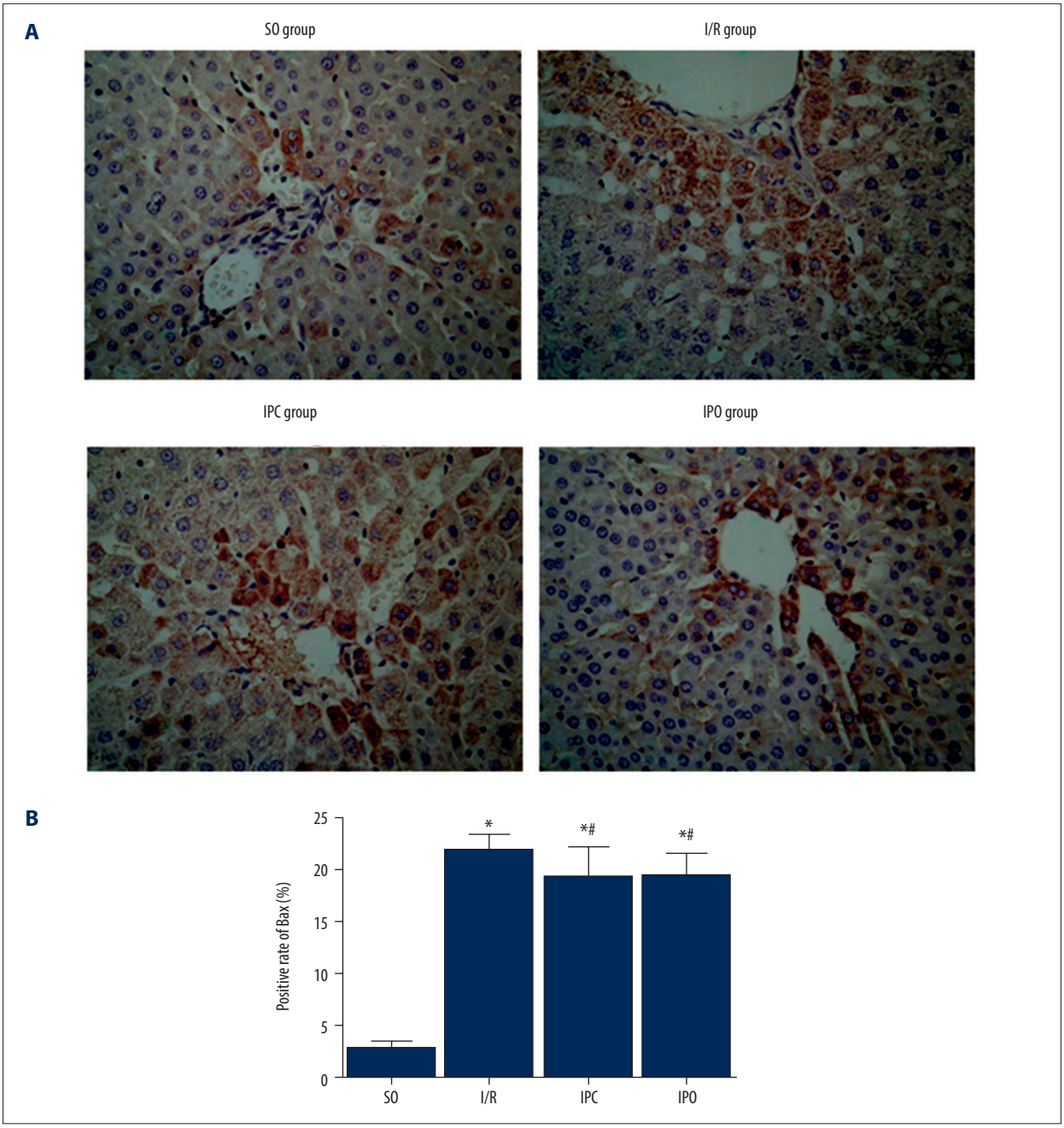

Figure 4. Level of Bax protein in liver tissue. Rats were divided into the SO group, I/R group, IPC group, and IPO group. Bax level was detected with immunohistochemistry. (**A**) Representative immunohistochemical staining results of Bax in SO group, I/R group, IPC group, and IPO group are shown. (**B**) Positive rate of Bax. Compared with SO, * P<0.05; compared with I/R, # P<0.05.

compared with the SO group, the level of Bcl-2 protein in liver tissue of the I/R, IPC, and IPO groups was significantly increased (P<0.05) (Figure 3B). The level of Bcl-2 protein in IPO and IPC group was significantly higher than that in the I/R group (P<0.05), but there was no significant difference between the IPO group and IPC group (P>0.05).

Level of Bax protein in liver tissue

Immunohistochemistry was also used to detect Bax protein level in liver tissue. As shown in Figure 4A, the positive rate of Bax in the IPC group and IPO group was lower than that in the I/R group. Compared with the SO group, the level of Bax protein in liver tissue of the I/R, IPC, and IPO groups was significantly

Indexed in: [Current Contents/Clinical Medicine] [SCI Expanded] [ISI Alerting System] [ISI Journals Master List] [Index Medicus/MEDLINE] [EMBASE/Excerpta Medica] [Chemical Abstracts/CAS]

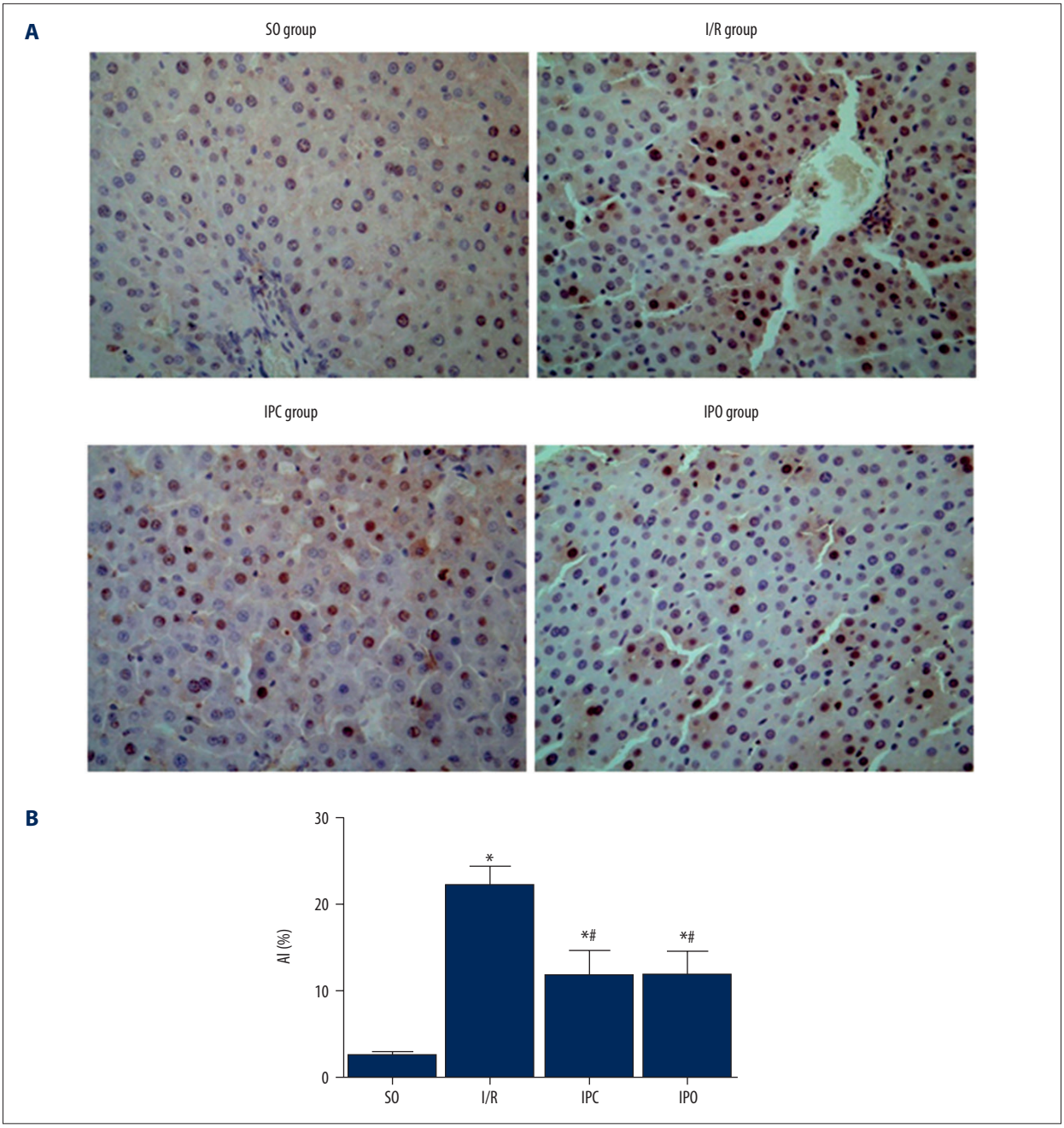

Figure 5. Apoptotic rate of hepatocytes in each group. Rats were divided into the SO group, I/R group, IPC group, and IPO group. Apoptosis was analyzed with TUNEL assay. (**A**) Representative TUNEL results of SO group, I/R group, IPC group, and IPO group are shown. (**B**) Analysis of apoptosis index. Compared with SO, * P<0.05; compared with I/R, # P<0.05.

increased (P<0.05). The level of Bax protein in the IPO and IPC group was significantly lower than that in the I/R group (P<0.05), but there was no significant difference between the IPO group and IPC group (P>0.05) (Figure 4B).

Apoptotic rate of hepatocytes in each group

To analyze cell apoptosis, TUNEL assay was performed. As shown in Figure 5A, the positive rate of apoptotic cells in the IPC group and IPO group was lower than that in the I/R group. As shown in Figure 5B, apoptosis index in the I/R, IPC, and IPO groups was significantly higher than in the SO group (P<0.05). Compared with the I/R group, the apoptosis index decreased

Indexed in: [Current Contents/Clinical Medicine] [SCI Expanded] [ISI Alerting System] [ISI Journals Master List] [Index Medicus/MEDLINE] [EMBASE/Excerpta Medica] [Chemical Abstracts/CAS]

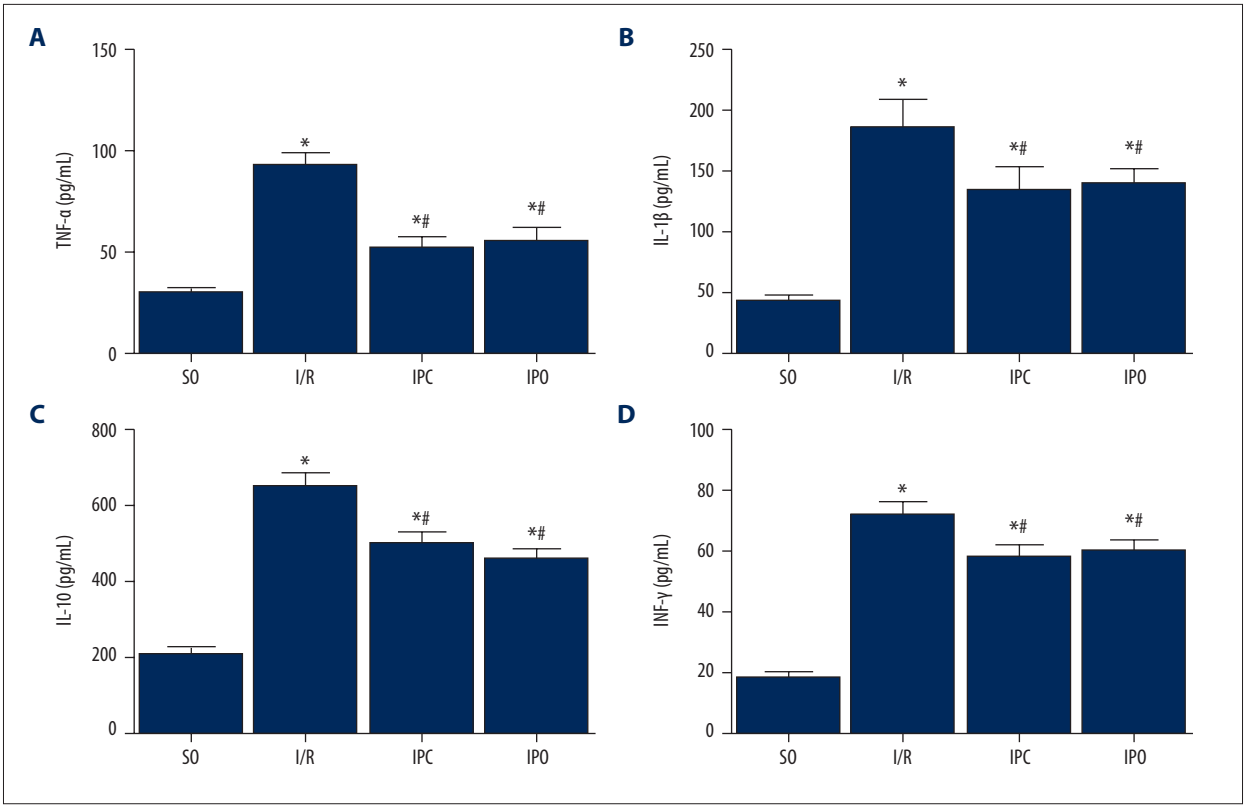

Figure 6. Changes in expression level of inflammatory factors in liver tissue. Rats were divided into the SO group, I/R group, IPC group, and IPO group. The levels of (**A**) TNF-α, (**B**) IL-1β, (**C**) IL-10, and (**D**) INF-γ in liver tissue were detected with ELISA. Compared with SO, * P<0.05; compared with I/R, # P<0.05.

significantly in the IPO and IPC groups (P<0.05). However, no significant difference was observed between the IPO and IPC groups (P>0.05).

Changes of expression level of inflammatory factors in liver tissue

ELISA was used to detect cytokine levels in liver tissues. The expression levels of TNF-α (Figure 6A), IL-1β (Figure 6B), IL-10 (Figure 6C), and INF-γ (Figure 6D) in liver tissues of the I/R, IPC, and IPO groups were significantly higher than those in the SO group (P<0.05). Compared with the I/R group, the expression levels of TNF-α, IL-1β, IL-10, and INF-γ in liver tissue of the IPO and IPC groups were significantly lower (P<0.05). However, no significant difference was found between the IPO group and IPC group (P>0.05).

Ultrastructural changes of hepatocytes in each group were observed under electron microscopy

Ultrastructural changes of hepatocytes were observed under an electron microscope. In the SO group, the nuclear membrane of hepatocytes was normal. The distribution of mitochondria was uniform and the size was normal (Figure 7A1, 7A2). In the I/R group, infiltration of neutrophils and exudation of red blood cells were observed in liver tissue, and the deformation of hepatocyte membrane and nuclear membrane was severe. The nuclear heterochromatin was obviously concentrated, the nuclear membrane was thickened, the nucleolus was concentrated, and the euchromatin area was rough and flocculent. The mitochondria were obviously swollen, the number increased, the crest was broken, and the crest was obviously loose and dissolved, with a large number of vacuoles. The endoplasmic reticulum was dense, with irregular clusters. The Golgi apparatus and vesicles disappeared, and the ribosomes could not be distinguished (Figure 7B1, 7B2). The changes in the IPC group (Figure 7C1, 7C2) were similar to those in the IPO group (Figure 7D1, 7D2) – the ultrastructural damage of cells was significantly reduced, the morphology of hepatocytes was good, the membrane structure was basically intact, and there was less exudation of blood cells. There was no obvious neutrophil infiltration, the structure of mitochondria was basically normal, the matrix granules disappeared; and there was mild edema, dense ridges, and no vacuole formation.

Indexed in: [Current Contents/Clinical Medicine] [SCI Expanded] [ISI Alerting System] [ISI Journals Master List] [Index Medicus/MEDLINE] [EMBASE/Excerpta Medica] [Chemical Abstracts/CAS]

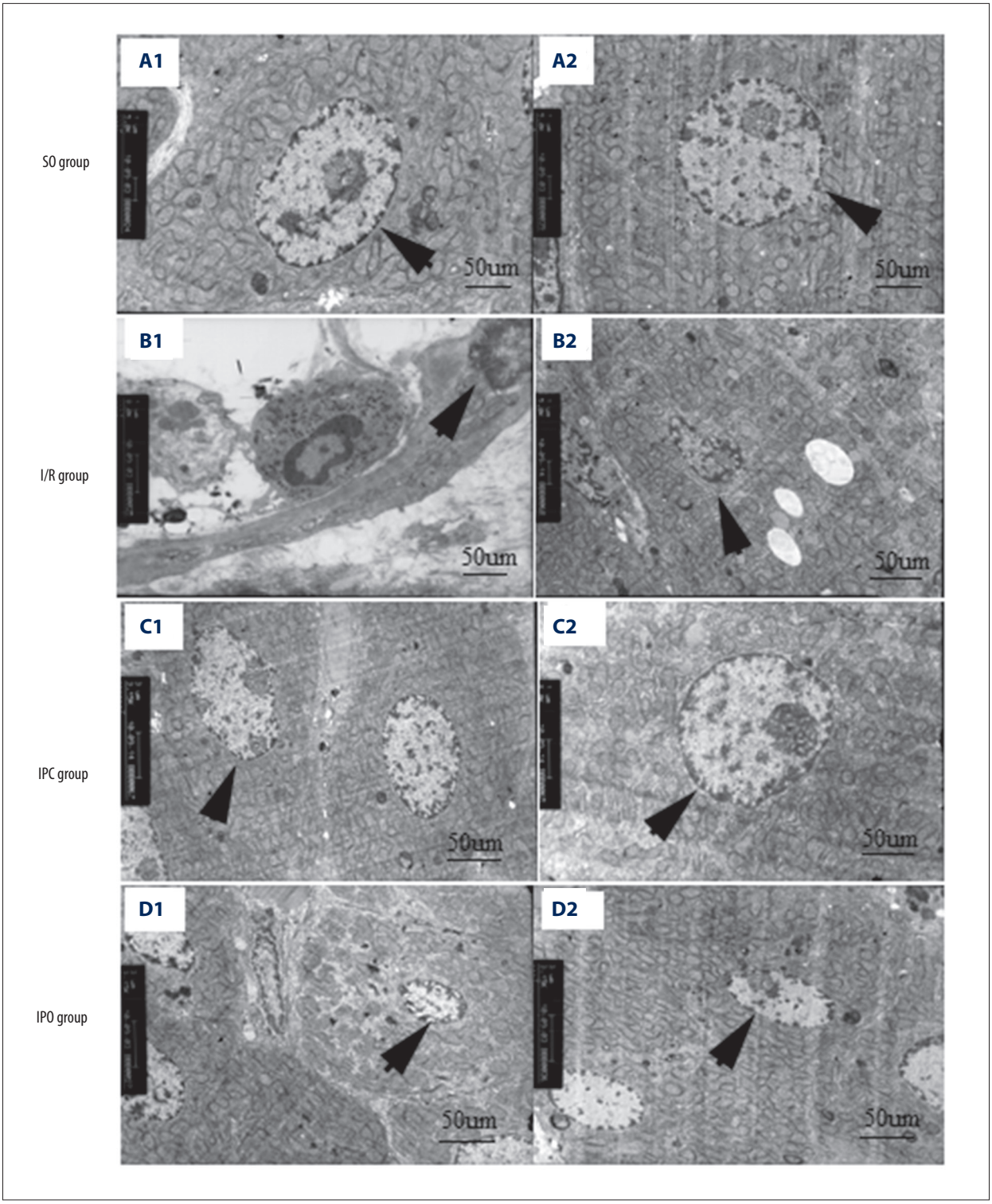

Figure 7. Ultrastructural changes of hepatocytes. Rats were divided into the SO group, I/R group, IPC group, and IPO group. Electron microscopy was used to observe the ultrastructural changes of hepatocytes in each group. SO group: **A1**×5.0k, **A2**×5.0k (arrows indicate the nuclei); I/R group: **B1**×8.0k, **B2**×5.0k (arrows indicate endoplasmic reticulum); IPC group: **C1**×3.15k, **C2**×8.0k (arrows indicate nuclei); IPO group: **D1**×3.15k, **D2**×3.15k (arrows indicate endoplasmic reticulum).

Indexed in: [Current Contents/Clinical Medicine] [SCI Expanded] [ISI Alerting System] [ISI Journals Master List] [Index Medicus/MEDLINE] [EMBASE/Excerpta Medica] [Chemical Abstracts/CAS]

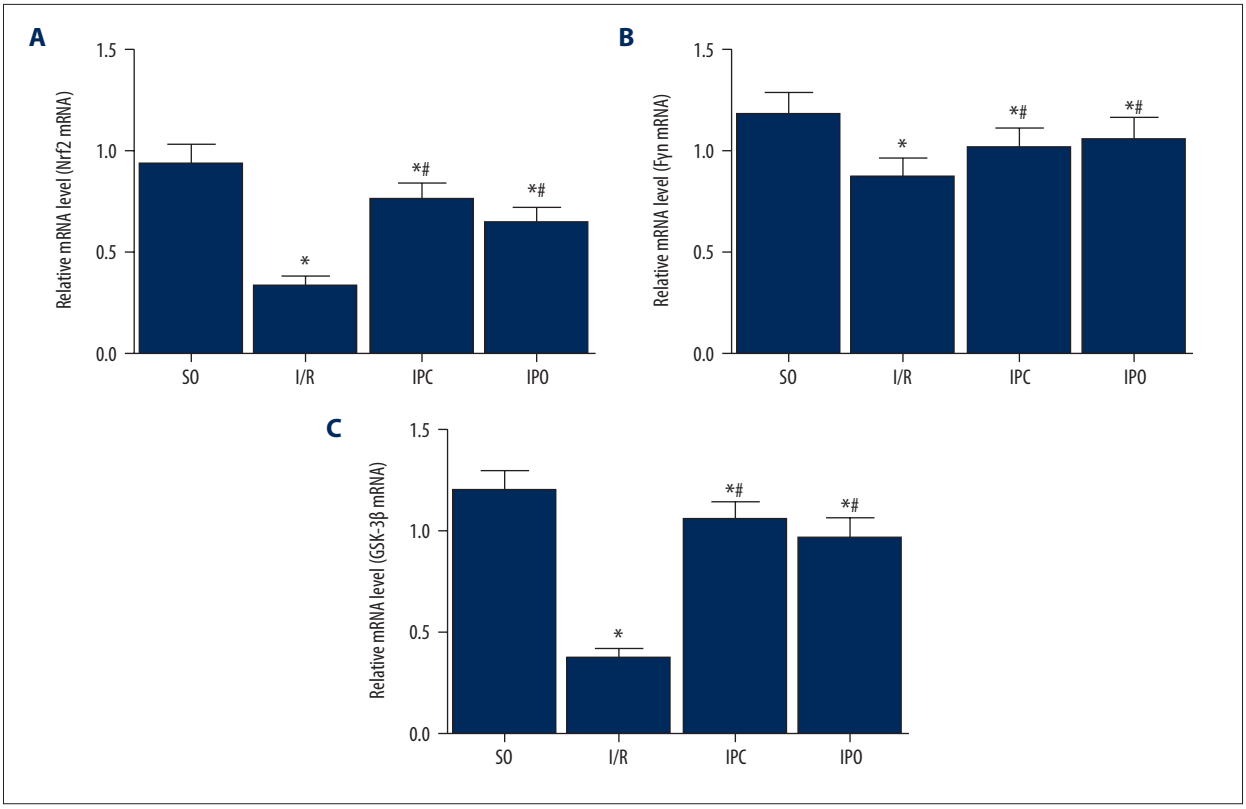

Figure 8. Analysis of GSK-3β/Fyn/Nrf2 mRNA expression in liver tissue. Rats were divided into the SO group, I/R group, IPC group, and IPO group. RT-qPCR was used to detect the mRNA levels of (**A**) Nrf2, (**B**) Fyn, and (**C**) GSK-3β in liver tissues. Compared with SO, * P<0.05; compared with I/R, # P<0.05.

Changes of GSK-3β/Fyn/Nrf2 mRNA expression in liver tissue

RT-qPCR was used to analyze mRNA expression. Compared with the SO group, the expression of Nrf2 (Figure 8A), Fyn (Figure 8B), and GSK-3β (Figure 8C) mRNA in liver tissue of the I/R, IPC, and IPO groups decreased significantly (P<0.05). Their expression levels in liver tissue of the IPO group and IPC group were significantly higher than those in the I/R group (P<0.05). However, there was no significant difference between the IPO group and IPC group (P>0.05).

Changes of GSK-3β/Fyn/Nrf2 protein level in liver tissue

To determine the protein changes, Western blot analysis was performed. The levels of Nrf2 (Figure 9A), Fyn (Figure 9B), and GSK-3β (Figure 9C) in liver tissues of the I/R, IPC, and IPO groups were significantly lower than in the SO group (P<0.05). Representative Western blot images are shown in Figure 9D. Compared with the I/R group, the levels of Nrf2, Fyn, and GSK-3β in liver tissue of the IPO group and IPC group were significantly higher (P<0.05). However, no significant difference was found between the IPO group and IPC group (P>0.05).

Discussion

ALT and AST are mainly distributed in liver and plasma. When hepatocytes are injured, ALT and AST increase, which are the main indicators of liver function [31]. SOD is an important antioxidant enzyme *in vivo* and can scavenge superoxide anion free radicals and prevent cell damage caused by membrane lipid peroxidation. MPO is a marker enzyme of PMN, and its activity can reflect the degree of PMN infiltration and the release of inflammatory mediators in liver tissue [32,33]. MDA is a product of lipid peroxidation and an index used to measure the degree of tissue peroxidation damage. LDH is a cytoplasmic enzyme, and its level in plasma can reflect the severity of tissue damage [34,35]. GSH-Px can catalyze the decomposition of hydrogen peroxide and protect cell membranes from cell damage [36,37]. CAT is an enzyme scavenger that can scavenge oxygen free radicals, strengthen the ability of antioxidation, and protect cells and the body [38]. The results in the present study showed that, compared with the SO group, the levels of SOD, GSH-Px, and CAT in liver tissue of the I/R, IPC, and IPO groups were significantly lower, while the levels of MDA, MPO, ROS, ALT, AST, ALP, and LDH were significantly higher in the I/R, IPC, and IPO groups (P<0.05). The levels of SOD, GSH-Px, and CAT in the IPO and IPC groups increased, while the

Indexed in: [Current Contents/Clinical Medicine] [SCI Expanded] [ISI Alerting System] [ISI Journals Master List] [Index Medicus/MEDLINE] [EMBASE/Excerpta Medica] [Chemical Abstracts/CAS]

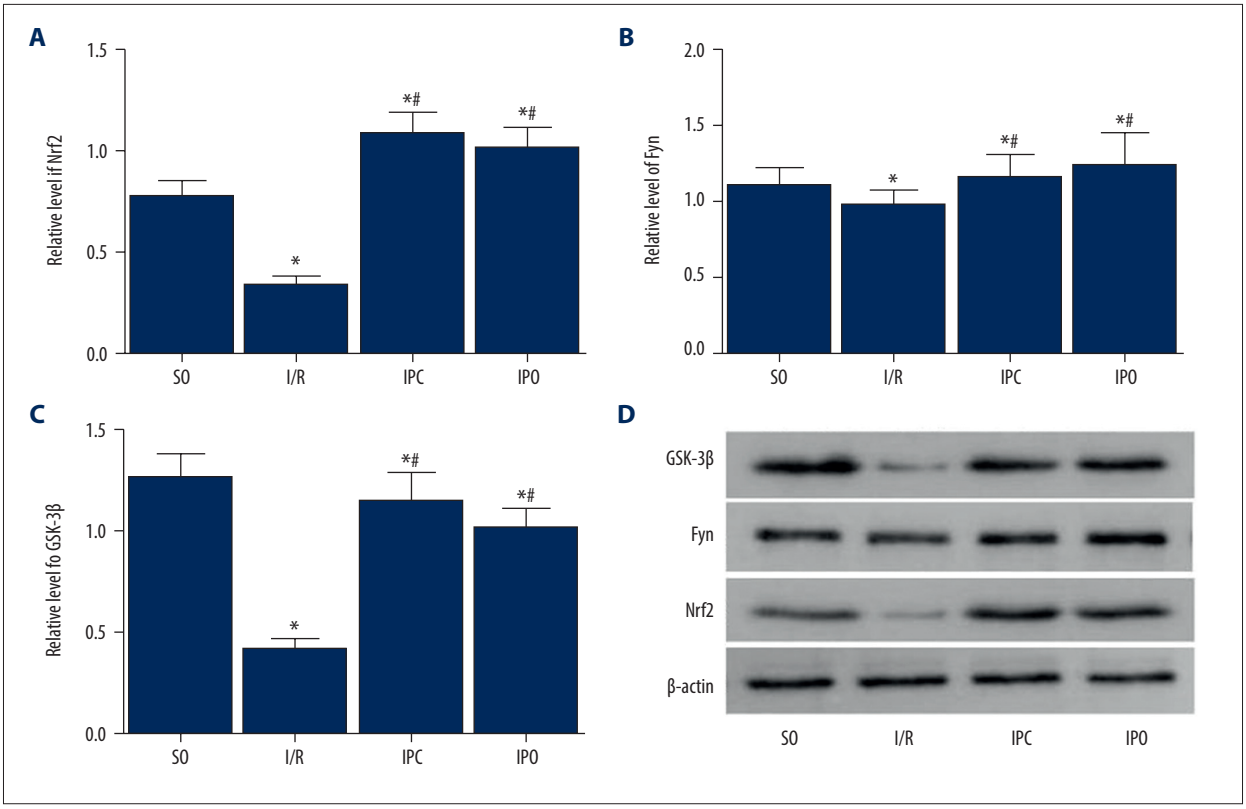

Figure 9. Analysis of GSK-3β/Fyn/Nrf2 protein levels in liver tissue. Rats were divided into the SO group, I/R group, IPC group, and IPO group. Western blot analysis was used to detect the protein levels. (**A–C**) Quantitative Western blot results of (**A**) Nrf2, (**B**) Fyn, and (**C**) GSK-3β in liver tissues are shown. (**D**) Representative Western blot results. Compared with SO, * P<0.05; compared with I/R, # P<0.05.

levels of MDA, MPO, ROS, ALT, AST, ALP, and LDH decreased significantly compared with those in the I/R group, but there was no significant difference between the IPO group and IPC group. In addition, compared with the SO group, the expression levels of TNF- α, IL-1 β, IL-10, and INF- γ were significantly increased in the I/R, IPC and IPO groups. The expression of TNF-α, IL-1 β, IL-10, and INF-γ in liver tissue of the IPO and IPC groups was significantly lower than that of the I/R group. There was no significant difference between the IPO group and IPC group. These results suggest that limb I/R can cause liver edema, increase production of free radicals, and cause neutrophil infiltration and severe liver function damage; however, IPO and IPC can regulate intracellular calcium stability, antilipid peroxidation and inflammation, and improve liver injury.

Cell apoptosis plays a very important role in limb I/R injury. The increase of oxygen free radicals, the enhancement of oxidative stress, the disturbance of energy metabolism, and the influx of Ca^{2+} into cells after limb I/R injury can increase the permeability of mitochondria. However, damage to the structure and function of mitochondria lead to ion homeostasis imbalance and mitochondrial uncoupling, which eventually leads to cell apoptosis [39–41]. The results of this study showed that the mitochondria of hepatocytes were evenly distributed and normal in th SO group, while neutrophils were infiltrated, red blood cells were exudative, mitochondria were obviously swollen, the number of mitochondria increased, cristae ruptured, crests were loosened and dissolved, and there were many vacuoles in the I/R group. In the IPC group and IPO group, the infiltration of neutrophils in hepatocytes was not obvious, the structure of mitochondria was basically normal, matrix granules disappeared, and there was mild edema, dense crests, and no vacuole formation. The Bc1-2 gene family is closely involved in apoptosis. The Bc1-2 gene, as a member of the Bc1-2 gene family, can promote cell survival and prolong cell life, and is thus called an “anti-apoptotic gene” [42]. The Bax gene is a member of the Bc1-2 gene family, and like the Bc1-2 gene it contains 3 homologous regions of BH1, BH2, and BH3. In contrast to Bcl-2, Bax is a pro-apoptotic gene and can promote the release of cytochrome C from mitochondria, thus promoting apoptosis. Bax can antagonize the inhibition of apoptosis mediated by Bc1-2 and accelerate the occurrence of apoptosis [43,44]. In this study, we found that, compared with the SO group, the levels of Bcl-2 and Bax proteins, hepatocyte apoptosis, and apoptosis index in the I/R, IPC, and IPO groups increased significantly. Compared with the I/R group,

Indexed in: [Current Contents/Clinical Medicine] [SCI Expanded] [ISI Alerting System] [ISI Journals Master List] [Index Medicus/MEDLINE] [EMBASE/Excerpta Medica] [Chemical Abstracts/CAS]

their levels decreased in the IPO and IPC groups. These results suggest that the protective effect of IPO on hepatic IR may occur through upregulating the level of Bcl-2 and downregulating the level of Bax, so as to reduce hepatocyte apoptosis.

Nrf2 is a leucine zipper transcription factor in the basic region, which regulates the expression of a series of oxidation-related genes. Nrf2 activation can induce the transcription of many protective genes such as NAD(P) Hquinone oxidoreductase 1, heme oxygenase 1, and glutamate cysteine ligase [45]. It can thus protect the body from harmful substances such as ROS, SOD, CAT, GSH-Px, carcinogens, and drug-active metabolites [46], thereby inhibiting the damage caused by various oxidative stimuli to the body [47,48]. Glycogen synthase kinase (GSK-3β) is a serine/tryptophan kinase involved in glycogen synthesis [49]. GSK-3β is involved in the occurrence and development of a variety of diseases [50]. GSK-3β has multiple active sites. When the complex amino acid site (Tyr216) is phosphorylated, its activity is increased, and when the amino terminal serine site (Ser9) site is phosphorylated, its activity is decreased. GSK-3β can regulate Nrf2 activity by Fyn and participate in the regulation of cellular oxidative stress [25,51,52]. Fyn is a member of the Scr tyrosine protein kinase family; after activation, it can enter the nucleus and exports out the nucleus Nrf2, which can be degraded by protease after ubiquitination [26]. Studies have shown that the Fyn signaling pathway plays an indispensable role in myelin formation by activating myelin basic protein [53,54]. Fyn is expressed in the nucleus, and its expression level is significantly decreased after hypoxia-ischemia [55]. Here, our results showed that, compared with the SO group, the expression of Nrf2, Fyn, and GSK-3β mRNA and their protein levels decreased significantly in liver tissue of the I/R group. Their levels in liver tissue of the IPO and IPC group were significantly higher than those in the I/R group. This suggests that IPO can alleviate the secondary liver injury and protect liver function after limb I/R, which may be achieved by regulating the GSK-3 β/Fyn/Nrf2 pathway. However, unlike previous studies [26,51,52,56], which suggested that GSK-3β is upstream of Fyn in regulating Nrf2 nuclear export and degradation, our study only preliminarily examined the changes of Nrf2, GSK-3β, and Fyn at mRNA and protein levels and did not reveal any specific relationship among GSK-3β, Fyn, and Nrf2. This is because we only detected the total level of Nrf2, but not the nuclear Nrf2, and we did not investigate the down-stream gene of Nrf2. This is a limitation of our study. In the future, we will carry out further studies with inhibitors or knockdown/knockout methods to reveal the details of the role of GSK-3beta/Fyn/Nrf2 pathway in I/R-induced liver injury and to demonstrate the relationships among GSK-3β, Fyn, and Nrf2.

Both IPC and IPO can exert protective effects against I/R-induced injury, but they may act through different mechanisms. For example, it is reported that in I/R, IPO has antiarrhythmic effects after reperfusion, while IPC has antiarrhythmic effects during ischemia [57]. In the present study, IPC was used as a positive control. Our results showed that both IPO and IPC had protective effects on the liver after hindlimb I/R. However, there was no significant difference between IPO and IPC. Further studies are needed to compare the effects and mechanisms of IPO and IPC on I/R-induced liver injury.

Conclusions

IPO can alleviate the liver injury and protect liver function following limb I/R. The possible mechanism is by reducing lipid peroxide reaction in lower-limb I/R, inhibit PMN infiltration, enhance the scavenging of oxygen free radicals, increase the level of Bcl-2 protein, and decrease the activity of Bax protein. These effects may be achieved by regulating the GSK-3β/Fyn/Nrf2 pathway. This study provides a theoretical basis for clinical mitigation of limb I/R injury and prevention of liver damage to protect liver function.

Conflict of interest

None.

References:

1. Yassin MM, Harkin DW, Barros D'Sa AA et al: Lower limb ischemia-reperfusion injury triggers a systemic inflammatory response and multiple organ dysfunction. World J Surg, 2002; 26: 115–21
2. Cai L, Li Y, Zhang Q et al: Salidroside protects rat liver against ischemia/reperfusion injury by regulating the GSK-3beta/Nrf2-dependent antioxidant response and mitochondrial permeability transition. Eur J Pharmacol, 2017; 806: 32–42
3. Ren Y, Wang LH, Deng FS et al: Protective effect and mechanism of alpha-lipoic acid on partial hepatic ischemia-reperfusion injury in adult male rats. Physiol Res, 2019; 68(5): 739–45
4. Vasques ER, Cunha JE, Coelho AM et al: Trisulfate disaccharide decreases calcium overload and protects liver injury secondary to liver ischemia/reperfusion. PLoS One, 2016; 11: e0149630
5. Vrakas G, Tsalis K, Roidos GN et al: Synergistic effect of ischemic preconditioning and antithrombin in ischemia-reperfusion injury. Exp Clin Transplant, 2017; 15: 320–28
6. Ni D, Wei H, Chen W et al: Ceria nanoparticles meet hepatic ischemia-reperfusion injury: The perfect imperfection. Adv Mater, 2019; 31(40): e1902956
7. Han JY, Li Q, Pan CS et al: Effects and mechanisms of QiShenYiQi pills and major ingredients on myocardial microcirculatory disturbance, cardiac injury and fibrosis induced by ischemia-reperfusion. Pharmacol Res, 2019; 147: 104386
8. Ojo OB, Amoo ZA, Saliu IO et al: Neurotherapeutic potential of kolaviron on neurotransmitter dysregulation, excitotoxicity, mitochondrial electron transport chain dysfunction and redox imbalance in 2-VO brain ischemia/reperfusion injury. Biomed Pharmacother, 2019; 111: 859–72

Indexed in: [Current Contents/Clinical Medicine] [SCI Expanded] [ISI Alerting System] [ISI Journals Master List] [Index Medicus/MEDLINE] [EMBASE/Excerpta Medica] [Chemical Abstracts/CAS]

9. Zhou Y, Gao G, Li Z et al: Protective effect of mitogen- and stress-activated protein kinase on the rats with focal ischemia-reperfusion injury. Inflammation, 2019; 42(6): 2159–69
10. Zhao YR, Lv WR, Zhou JL: Role of carbonyl sulfide in acute lung injury following limb ischemia/reperfusion in rats. Eur J Med Res, 2017; 22: 12
11. Zuluaga Tamayo M, Choudat L, Aid-Launais R et al: Astaxanthin complexes to attenuate muscle damage after *in vivo* femoral ischemia-reperfusion. Mar Drugs, 2019; 17(6): 354
12. Jaeschke H: Reactive oxygen and mechanisms of inflammatory liver injury: Present concepts. J Gastroenterol Hepatol, 2011; 26(Suppl. 1): 173–79
13. Zheng D, Li Z, Wei X et al: Role of miR-148a in mitigating hepatic ischemia-reperfusion injury by repressing the TLR4 signaling pathway via targeting CaMKIIalpha *in vivo* and *in vitro*. Cell Physiol Biochem, 2018; 49: 2060–72
14. Li X, Wu Y, Zhang W et al: Pre-conditioning with tanshinone IIA attenuates the ischemia/reperfusion injury caused by liver grafts via regulation of HMGB1 in rat Kupffer cells. Biomed Pharmacother, 2017; 89: 1392–400
15. Liu Y, Zhang W, Cheng Y et al: Activation of PPARgamma by curcumin protects mice from ischemia/reperfusion injury induced by orthotopic liver transplantation via modulating polarization of Kupffer cells. Int Immunopharmacol, 2018; 62: 270–76
16. Murry CE, Jennings RB, Reimer KA: Preconditioning with ischemia: A delay of lethal cell injury in ischemic myocardium. Circulation, 1986; 74: 1124–36
17. Kocman EA, Ozatik O, Sahin A et al: Effects of ischemic preconditioning protocols on skeletal muscle ischemia-reperfusion injury. J Surg Res, 2015; 193: 942–52
18. Hummitzsch L, Zitta K, Berndt R et al: Remote ischemic preconditioning attenuates intestinal mucosal damage: Insight from a rat model of ischemia-reperfusion injury. J Transl Med, 2019; 17: 136
19. Singh H, Kumar M, Singh N et al: Late phases of cardioprotection during remote ischemic preconditioning and adenosine preconditioning involve activation of neurogenic pathway. J Cardiovasc Pharmacol, 2019; 73: 63–69
20. Zhao ZQ, Corvera JS, Halkos ME et al: Inhibition of myocardial injury by ischemic postconditioning during reperfusion: Comparison with ischemic preconditioning. Am J Physiol, 2003; 285: H579–88
21. Figueira ERR, Rocha-Filho JA, Lanchotte C et al: Sevoflurane preconditioning plus postconditioning decreases inflammatory response with hemodynamic recovery in experimental liver ischemia reperfusion. Gastroenterol Res Pract, 2019; 2019: 5758984
22. Kontis E, Pantiora E, Melemeni A et al: Ischemic postconditioning decreases iNOS gene expression but ischemic preconditioning ameliorates histological injury in a swine model of extended liver resection. Transl Gastroenterol Hepatol, 2019; 4: 5
23. Liu J, Wu KC, Lu YF et al: Nrf2 protection against liver injury produced by various hepatotoxicants. Oxid Med Cell Longev, 2013; 2013: 305861
24. Done AJ, Traustadottir T: Nrf2 mediates redox adaptations to exercise. Redox Biol, 2016; 10: 191–99
25. Theeuwes WF, Gosker HR, Langen RCJ et al: Inactivation of glycogen synthase kinase 3beta (GSK-3beta) enhances mitochondrial biogenesis during myogenesis. Biochim Biophys Acta Mol Basis Dis, 2018; 1864: 2913–26
26. Mittal SPK, Khole S, Jagadish N et al: Andrographolide protects liver cells from H2O2 induced cell death by upregulation of Nrf-2/HO-1 mediated via adenosine A2a receptor signalling. Biochim Biophys Acta, 2016; 1860: 2377–90
27. Zheng D, Liu Z, Zhou Y et al: Urolithin B, a gut microbiota metabolite, protects against myocardial ischemia/reperfusion injury via p62/Keap1/Nrf2 signaling pathway. Pharmacol Res, 2020; 153: 104655
28. Velez DE, Mestre-Cordero VE, Hermann R et al: Rosuvastatin protects isolated hearts against ischemia-reperfusion injury: Role of Akt-GSK-3beta, metabolic environment, and mitochondrial permeability transition pore. J Physiol Biochem, 2020; 76: 85–98
29. Hao L, Wei X, Guo P et al: Neuroprotective effects of Inhibiting Fyn S-nitrosylation on cerebral ischemia/reperfusion-induced damage to CA1 hippocampal neurons. Int J Mol Sci, 2016; 17: 1100
30. Kuntscher MV, Kastell T, Engel H et al: Late remote ischemic preconditioning in rat muscle and adipocutaneous flap models. Ann Plast Surg, 2003; 51: 84–90
31. Wu YL, Li ZL, Zhang XB et al: Yinchenhao decoction attenuates obstructive jaundice-induced liver injury and hepatocyte apoptosis by suppressing protein kinase RNA-like endoplasmic reticulum kinase-induced pathway. World J Gastroenterol, 2019; 25: 6205–21
32. Xue BB, Chen BH, Tang YN et al: Dexmedetomidine protects against lung injury induced by limb ischemia-reperfusion via the TLR4/MyD88/NF-kappaB pathway. Kaohsiung J Med Sci, 2019; 35: 672–78
33. Inan B, Sönmez Ergün S, Nurten A et al: Effects of cilostazol and diltiazem hydrochloride on ischemia-reperfusion injury in a rat hindlimb model. Heart Surg Forum, 2017; 20: E058–65
34. Ye Y, Shan Y, Bao C et al: Ginsenoside Rg1 protects against hind-limb ischemia reperfusion induced lung injury via NF-kappaB/COX-2 signaling pathway. Int Immunopharmacol, 2018; 60: 96–103
35. Zhang Y, Li C, Zhang H et al: Color-coded digital subtraction angiography for assessing acute skeletal muscle ischemia-reperfusion injury in a rabbit model. Acad Radiol, 2018; 25: 1609–16
36. Nong K, Wang W, Niu X et al: Hepatoprotective effect of exosomes from human-induced pluripotent stem cell-derived mesenchymal stromal cells against hepatic ischemia-reperfusion injury in rats. Cytotherapy, 2016; 18: 1548–59
37. Sirmali R, Armağan A, Öktem F et al: Protective effects of erdosteine, vitamin E, and vitamin C on renal injury induced by the ischemia-reperfusion of the hind limbs in rats. Turk J Med Sci, 2015; 45: 33–37
38. Batinic-Haberle I, Tovmasyan A, Roberts ER et al: SOD therapeutics: Latest insights into their structure-activity relationships and impact on the cellular redox-based signaling pathways. Antioxid Redox Signal, 2014; 20: 2372–415
39. Chang JC, Lien CF, Lee WS et al: Intermittent hypoxia prevents myocardial mitochondrial Ca(2+) overload and cell death during ischemia/reperfusion: The role of reactive oxygen species. Cells, 2019; 8: 564
40. Andrienko T, Pasdois P, Rossbach A et al: Real-time fluorescence measurements of ROS and [Ca2+] in ischemic/reperfused rat hearts: Detectable increases occur only after mitochondrial pore opening and are attenuated by ischemic preconditioning. PLoS One, 2016; 11: e0167300
41. Ji ZP, Li YX, Shi BX et al: Hypoxia preconditioning protects Ca(2+)-ATPase activation of intestinal mucosal cells against R/I injury in a rat liver transplantation model. World J Gastroenterol, 2018; 24: 360–70
42. Chen J, Li X, Qiu J et al: Kinetics of apoptosis and expression of apoptosis-related proteins in rat CA3 hippocampus cells after experimental diffuse brain injury. Cell Biochem Biophys, 2013; 67: 1015–19
43. Krajewski S, Krajewska M, Shabaik A et al: Immunohistochemical determination of *in vivo* distribution of Bax, a dominant inhibitor of Bcl-2. Am J Pathol, 1994; 145: 1323–36
44. Imahashi K, Schneider MD, Steenbergen C et al: Transgenic expression of Bcl-2 modulates energy metabolism, prevents cytosolic acidification during ischemia, and reduces ischemia/reperfusion injury. Circ Res, 2004; 95: 734–41
45. Hybertson BM, Gao B, Bose SK et al: Oxidative stress in health and disease: The therapeutic potential of Nrf2 activation. Mol Aspects Med, 2011; 32: 234–46
46. Kobayashi M, Yamamoto M: Nrf2-Keap1 regulation of cellular defense mechanisms against electrophiles and reactive oxygen species. Adv Enzyme Regul, 2006; 46: 113–40
47. Wu Q, Zhang D, Tao N et al: Induction of Nrf2 and metallothionein as a common mechanism of hepatoprotective medicinal herbs. Am J Chin Med, 2014; 42: 207–21
48. Peng X, Dai C, Liu Q et al: Curcumin attenuates on carbon tetrachloride-induced acute liver injury in mice via modulation of the Nrf2/HO-1 and TGF-beta1/Smad3 pathway. Molecules, 2018; 23: 215
49. Kockeritz L, Doble B, Patel S et al: Glycogen synthase kinase-3 – an overview of an over-achieving protein kinase. Curr Drug Targets, 2006; 7: 1377–88
50. Guo J, Xia NN, Yang LL et al: GSK-3beta and vitamin D receptor are involved in beta-catenin and snail signaling in high glucose-induced epithelial-mesenchymal transition of mouse podocytes. Cell Physiol Biochem, 2014; 33: 1087–96
51. Zhang HF, Wang HJ, Wang YL et al: Salvianolic acid a protects the kidney against oxidative stress by activating the Akt/GSK-3beta/Nrf2 signaling pathway and inhibiting the NF-kappaB signaling pathway in 5/6 nephrectomized rats. Oxid Med Cell Longev, 2019; 2019: 2853534
52. Cuadrado A: Structural and functional characterization of Nrf2 degradation by glycogen synthase kinase 3/beta-TrCP. Free Radic Biol Med, 2015; 88: 147–57
53. Colognato H, Ramachandrappa S, Olsen IM et al: Integrins direct Src family kinases to regulate distinct phases of oligodendrocyte development. J Cell Biol, 2004; 167: 365–75

Indexed in: [Current Contents/Clinical Medicine] [SCI Expanded] [ISI Alerting System] [ISI Journals Master List] [Index Medicus/MEDLINE] [EMBASE/Excerpta Medica] [Chemical Abstracts/CAS]

54. Gonsalvez D, Ferner AH, Peckham H et al: The roles of extracellular related-kinases 1 and 2 signaling in CNS myelination. Neuropharmacology, 2016; 110: 586–93
55. Knox R, Zhao C, Miguel-Perez D et al: Enhanced NMDA receptor tyrosine phosphorylation and increased brain injury following neonatal hypoxia-ischemia in mice with neuronal Fyn overexpression. Neurobiol Dis, 2013; 51: 113–19
56. Jain AK, Jaiswal AK: GSK-3beta acts upstream of Fyn kinase in regulation of nuclear export and degradation of NF-E2 related factor 2. J Biol Chem, 2007; 282: 16502–10
57. Spannbauer A, Traxler D, Lukovic D et al: Effect of ischemic preconditioning and postconditioning on exosome-rich fraction microRNA levels, in relation with electrophysiological parameters and ventricular arrhythmia in experimental closed-chest reperfused myocardial infarction. Int J Mol Sci, 2019; 20: 2140

Indexed in: [Current Contents/Clinical Medicine] [SCI Expanded] [ISI Alerting System] [ISI Journals Master List] [Index Medicus/MEDLINE] [EMBASE/Excerpta Medica] [Chemical Abstracts/CAS]